CFD NUMERICAL SIMULATION OF TEMPERATURE AND AIRFLOW DISTRIBUTION IN PIGSTY BASED ON GRID INDEPENDENCE VERIFICATION
/
基于网格独立性验证的猪舍温度和气流分布的CFD 数值模拟

Min Jin, Chunguang Wang*, Pengpeng Wang [1]
College of Mechanical and Electrical Engineering, Inner Mongolia Agricultural University, Hohhot, China
Tel: +86 18848110474; E-mail: imauwcg@126.com

DOI: https://doi.org/10.35633/inmateh-61-27

Keywords: *CFD, numerical simulation, grid independence, airflow velocity, temperature distribution*

ABSTRACT

Grid independence verification was implemented to improve the reliability of CFD numerical simulation in pigsty. The effects of four different grid numbers on airflow and temperature simulation of 0.4m, 1.0m and 1.6m heights were compared. The results showed that the third method of mesh generation and the grid numbers about 2.09 million were more suitable for this pigsty model. The average relative error of airflow velocity and temperature between the simulated and the measured alues were 7.1% and 3.8% respectively, the average NMSE were 0.0012 and 0.0066 respectively. Therefore, grid independence verification is of great significance for CFD numerical simulation.

摘要

为了提高猪舍 CFD 数值模拟的可靠性，对猪舍网格独立性进行了验证。比较了四种不同网格数对 0.4m、1.0m 和 1.6m 高度的气流和温度场模拟的影响。结果表明,第三种网格生成的方法和大约 209 万的网格数量更适合该猪舍模型。气流速度、温度的模拟值和实测值的平均相对误差分别为 7.1%和 3.8%,均方误差分别为 0.0012 和 0.0066。可见，网格独立性验证对提高 CFD 数值模拟的可靠性具有重要的意义。

INTRODUCTION

With the rapid development of large-scale and intensive pig husbandry, higher requirements have been put forward for the environment in pigsty. Temperature and airflow velocity are two of the most important environmental factors in pig farming which are directly related to the economic benefits and pigs' welfare. So, it is necessary to evaluate the environmental indexes efficiently and provide a comfortable environment for the pigs.

There are three main methods to study the airflow and temperature distributions in livestock buildings: field test, laboratory test (or wind tunnel test) and Computational Fluid Dynamics (CFD) numerical simulation *(Hong et al., 2013; Nielsen., 2015; Ntinas., 2017)*. Although the field test should be closer to the real conditions in the pigsty, it is easily affected by the external environment and the accuracy of the sensors. As for the laboratory test (wind tunnel test), under stable conditions, it can work better while requiring a lot of time and cost to repeat the different structural configurations and different weather conditions. CFD offers a feasible way to overcome the shortcomings of these two methods mentioned above; it has been widely used to study airflow and temperature distribution within livestock buildings *(Nielsen et al., 2015; Rojano et al., 2016; Sejun et al., 2014; Sapounas et al., 2013;)*. However, due to the heavy workload of mesh generation, the accuracy and efficiency of the simulation are all greatly affected by the gird numbers and the mesh quality (*Yao et al., 2016; Li et al., 2018)*. The impact of three mesh types (hexahedral, tetrahedral, and hybrid) and five grid numbers on the accuracy and computing costs of air distribution simulations has been conducted in a first-class aircraft cabin; the results showed that the hexahedral meshes can get the best result but also the highest computing costs (*Duan et al., 2015)*. Yu et al. investigated the computational accuracies and convergence rates of triangular and quadrilateral meshes, they concluded that the number of triangular meshes needs to be 4/3 times that of quadrilateral to obtain similar accuracy *(Yu et al., 2012).*

[1] *Min Jin, Ph.D. Stud. Eng.; Chunguang Wang*, Prof. Ph.D. Eng.; Pengpeng Wang , Ms. Stud. Eng.*

The effect of airflow velocity on heat exchange between cows' standing and tilting was also studied by CFD numerical simulation; the results indicated that CFD can be used as a useful way to get ideal results based on optimal parameters and reasonable mesh model *(Wang et al., 2018)*.

Therefore, prior to conduct the numerical simulation of the pigsty, grid independence verification must be done to minimize the workload of the mesh generation while not affecting the reliability and the accuracy of the results. In this study, field test and CFD numerical simulation are combined to verify the importance of grid independence test for improving the reliability of CFD numerical simulation in pigsty.

MATERIALS AND METHODS

- **Data source**

The experiment was carried out on a pig farm in Hohhot, Inner Mongolia, China (40°40 '26 "N, 111°21' 46"E). The dimensions of the pigsty are 9.2m (length) × 9.0m (width) × 3.6m (height), with negative pressure ventilation. There are 14 adjustable air inlets (265mm×655mm) at the top of the pigsty, many conveying pipes in the upper space, 2 automatic feeding equipment on the left side, 4 cylindrical finned heating pipes, 2 variable speed fans on the side walls and a 2m deep manure pit beneath the floor. Meanwhile, each pen is surrounded by solid wall and partially slatted concrete floor. The internal structure of the experimental pigsty is demonstrated in Fig.1.

The field test was conducted on January 9, 2018. The environmental temperature was measured and recorded by temperature sensors (HSTL-102WS, China) every 2s. In addition, an intelligent hot wire anemometer (9565-P, TSI, USA) was used to measure the air velocity every 0.2 s and averaged per second for a measurement period of 60s at each measuring point. As shown in Fig.2, the sensors were located in the centre of each pig pen as well as middle of the aisle at 3 different heights: 0.4m (height of lying pig), 1m (height of standing pig) and 1.6m (height of breeder). The 14 adjustable air inlets were set as the velocity inlets and the four outlets set as pressure outlets in GAMBIT. The heating was regarded as a constant heat source in the pigsty and its averaged surface temperature was measured by the infrared thermometer (MT4, Raytek, American) every 5min. Pigs' model was regarded as non-slip wall with constant temperature. In addition, the density of the pigs was 1100 kg.m^3, the specific heat was 3500 J.(kg.K)$^{-1}$ and the thermal conductivity as 0.464 W (m.K)$^{-1}$.

Fig. 1 - Internal structure of the pigsty

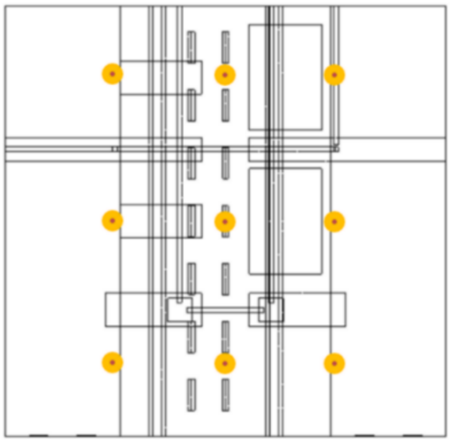

Fig. 2 - Sensor layout scheme in the pigsty

- **Numerical simulation**

➢ **Selection of governing equation**

No matter complex or simple the fluid flow is governed by the law of conservation. The basic conservation law mainly includes the mass conservation law, the momentum conservation law, energy conservation law, collectively known as the governing equation. In terms of the control equation of CFD, the continuity equation, the momentum equation and the energy equation are mainly applied (*Osorio Saraz et al., 2013*):

(1) Continuity equation:

$$\frac{\partial(\rho u)}{\partial x}+\frac{\partial(\rho v)}{\partial y}+\frac{\partial(\rho w)}{\partial z}=0 \tag{1}$$

where:

ρ is density. u, v and w are the components of the velocity vector in the direction of x, y and z.

(2) Momentum equation:

$$\frac{\partial(\rho\phi)}{\partial t}+div(\rho u\phi)=div(\Gamma grad\phi)+S \tag{2}$$

where:

ϕ is general variable, which can represent u, v and w.

Γ is the diffusion coefficient. S is the source item.

(3) Energy equation

$$\frac{\partial(\rho T)}{\partial t}+div(\rho uT)=div\left(\frac{k}{c_p}gradT\right)+S_T \tag{3}$$

where:

c_p is specific heat capacity, T is temperature [°C],

k is the heat transfer coefficient of the fluid and S_T is viscous dissipation term.

➢ **Selection of boundary condition**

The boundary condition is the prerequisites for the solution of the governing equation. Setting boundary condition includes selecting the simulation state, turbulence model and initial conditions.

The steady-state simulation based on pressure is employed in this study since the external climate of the pigsty is stable and the fan is running normally. Then, the renormalization group model (RNG $k-\varepsilon$ Model) is adopted as the turbulence model, which is a basic method that has been commonly used in current turbulence simulation studies with high accuracy and applicability. Besides, air is simplified as the stable and incompressible ideal air because of the fluctuations in airflow velocity and temperature are small. Meanwhile, considering the impact of gravity, the acceleration in the direction of gravity was set as -9.8m·s^{-2} and the material parameters of wall and the actual measured initial condition values are shown in Table 1 and Table 2, respectively. Moreover, in order to reduce the mesh numbers, the slatted floor is treated as a porous medium with 2cm width of the slot and 12 cm width of the slat. The inertial drag coefficient in X, Y and Z directions is 80m^{-1}, 1.2×10^{4} m^{-1} and 1.5×10^{2} m^{-1}, respectively and the viscous drag coefficient is 1.0×10^{5} m^{-2}, 1.6×10^{7}m^{-2}, 1.2×10^{5} m^{-2}, respectively. Then, the porosity of the slatted floor is calculated to be 0.14 by formula (4):

$$\frac{\Delta P}{l}=0.5\cdot R_1\cdot\rho_{air}\cdot v_2+\mu_{air}\cdot R_2 \tag{4}$$

where:

$\frac{\Delta P}{l}$ is the pressure drop per unit length of porous medium [$Pa.m^{-1}$]. R_1 is the inertial drag coefficient [m^{-1}], R_2 is the viscous drag coefficient [m^{-2}], ρ_{air} is the air density [$kg\cdot m^{-3}$], v is the velocity of air passing through in the porous medium [$m.s^{-1}$], μ_{air} is the velocity coefficient [$kg\cdot(m\cdot s^{-1})$].

Table 1

Wall material parameters

Parameter	Density [$kg\cdot m^{-3}$]	Specific heat capacity [$J\cdot(kg\cdot K)^{-1}$]	Heat conductivity coefficient [$W\cdot(m\cdot K)^{-1}$]
Brick wall	2000	920	0.81
Floor	1800	900	1.9
Roof	1050	1300	0.08

Table 2

Initial condition values

Parameter	Object	Measured values
Surface temperature [°C]	Front wall	7.4
	Back wall	8.0
	Left wall	6.4
	Right wall	5.8
	Roof	15.0
	Floor	5.0
Temperature [°C]	Pig	25.0
	Heating	30.0
	Outdoor temperature	-6.0
Velocity [m/s]	Air inlet	0.5

Additionally, to ensure the accuracy of CFD numerical simulation, the actual structure and configuration of the pigsty are kept as much as possible. The railings diameters are small with spacing of 0.1m, which have little effect on the simulation results, so they are not included in the CFD modelling while the shared feeders, the feeding equipment and the pipes in the upper space of the pigsty cannot be ignored because of their larger volumes.

As for pigs, they not only influence the air diffusion but also the temperature distribution. As shown in Fig.3, due to the low temperature in winter, the pigs were huddled together most of the time. Therefore, a cuboid with similar volume of the actual size of the space occupied by the pigs is used instead of multiple cuboids models, which greatly reduce the complexity of mesh partition and the computation cost.

Fig. 3 - Actual status of the pigs

RESULTS

- **Grid independence verification**

Gambit 2.4.6 is employed to establish the pigsty model (Fig.4). The effects of grid numbers are studied by adopting different meshing strategies in different computing domains with hybrid grids under four different densities. The numbers of mesh are 273,423 (represented by letter "A"), 1,648,998 ("B"), 2,090,991 "C"), 3,149,854 ("D") and the worst mesh quality is less than 0.97, which means that the meshing is reasonable and available. Fig.5 is one of the mesh models.

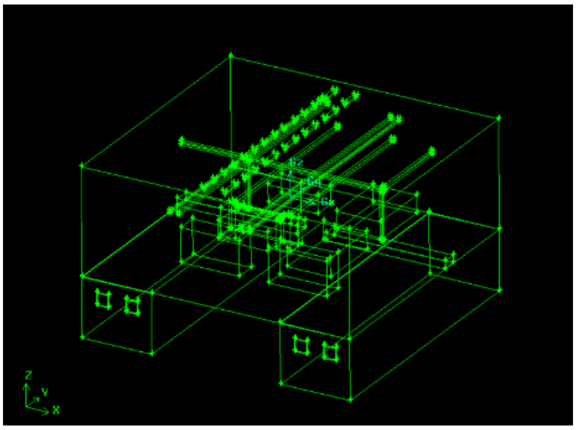

Fig. 4 – 3D model of the Pigsty

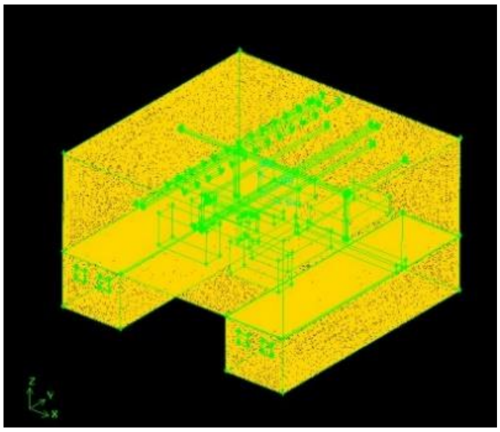

Fig. 5 - Mesh model of the Pigsty

The comparisons of the simulated values of the four different grid numbers A, B, C and D with the actual measured values at different height in the pigsty are presented in Fig.6-11.

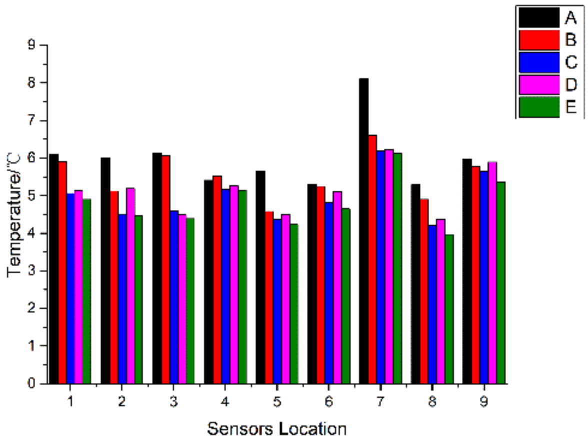

Fig. 6 - Airflow velocity values at height of 0.4m in pigsty

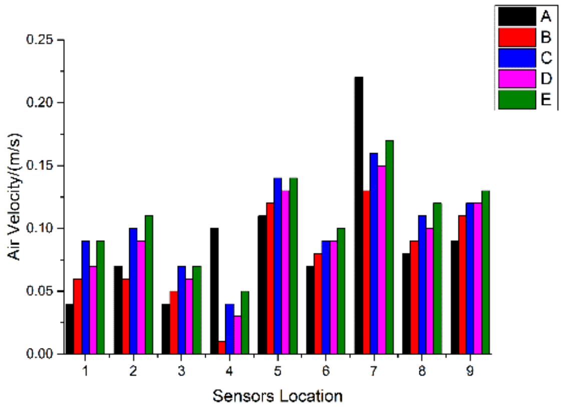

Fig. 7 - Temperature values at height of 0.4m in pigsty

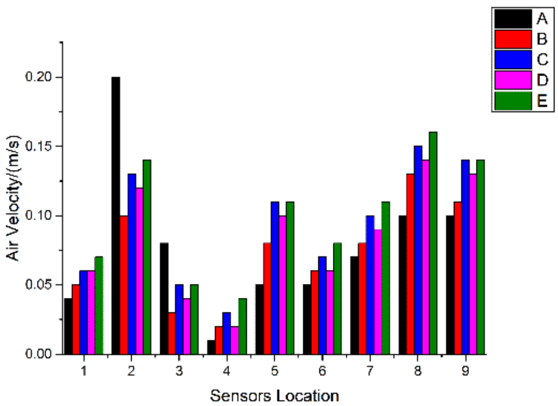

Fig. 8 - Airflow velocity values at height of 1m in pigsty

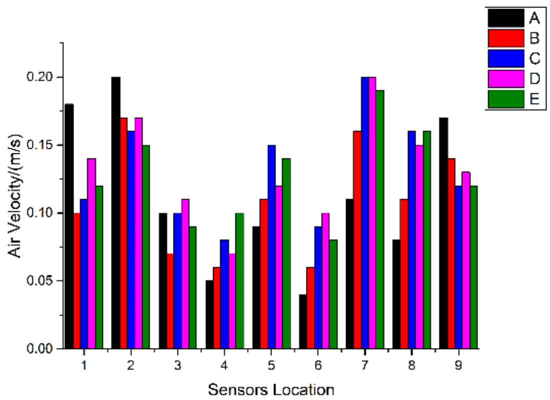

Fig. 9 - Temperature values at height of 1m in pigsty

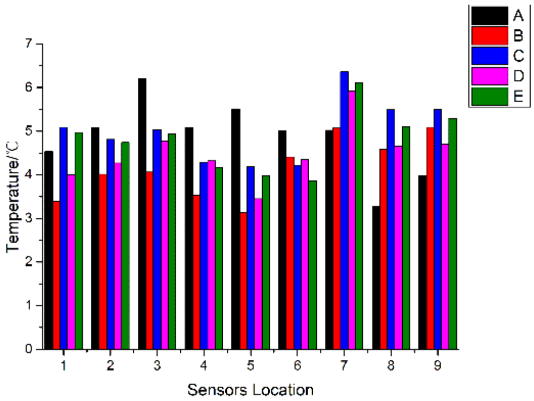

Fig. 10 - Airflow velocity values at height of 1.6m in pigsty (left)

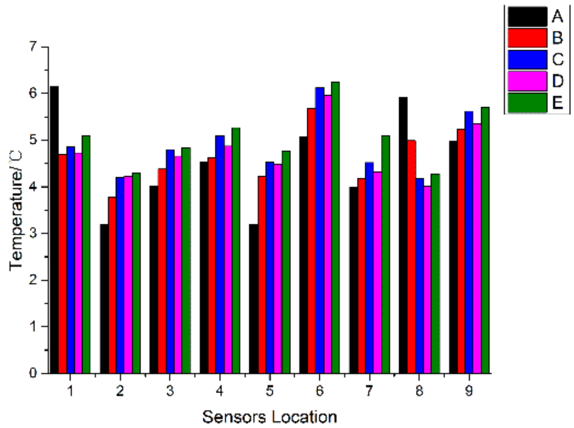

Fig. 11 - Temperature values at height of 1.6m in pigsty (right)

It can be found that grid numbers have great impacts on the accuracy of the simulation results. When the grid numbers are less than 1.64 million, there are large deviations between the simulation results and the measured values. When the grid numbers reached about 2.09 million and 3.14 million, the simulation results are all close to the measured values, but the former is more accurate. Meanwhile, the average relative error of airflow velocity of the four different grid numbers at different heights are presented in Table 3. The average relative error of temperature of the four different grid numbers at the 3 heights are 23.7%, 14.5%, 3.8% and 7.6%, respectively. When the grid numbers reached about 2.09 million, the simulated values are fit well with the actual measured values, and the relative errors of airflow velocity and temperature are the lowest. Then, continuing dividing the grids to 3.15 million, the results indicated that the relative error of airflow velocity and temperature increased by 9.9% and 3.8% compared to the 2.09 million grid number and the time cost is also obviously longer than the previous one. This is because with the mesh encryption, the discrete error decreases while the number of discrete points increase, which leads to the increase of rounding error of the simulation.

Table 3

Relative error at different heights with different grid numbers (%)

	A		B		C		D	
	V	T	V	T	V	T	V	T
0.4 m	48.1	22.3	31.7	11.6	6.8	3.8	16.4	6.4
1.0 m	50.7	25.4	32.0	15.7	6.6	3.3	18.8	7.0
1.6 m	40.4	23.4	22.5	16.3	7.9	4.3	15.7	9.4
Average	46.4	23.7	28.7	14.5	7.1	3.8	17.0	7.6

In order to further analyse the accuracy and reliability of the four mesh schemes, Normalized Mean Square Error (NMSE) is applied to judge the model performance (*Ntinas et al., 2017)*. NMSE is defined as follows:

$$NMSE=\frac{\left(\overline{c_s-c_m}\right)^2}{c_{sm}\cdot c_{om}} \tag{4}$$

$$\left(\overline{c_s-c_m}\right)^2=\frac{\sum_n\left(c_{si}-c_{mi}\right)^2}{c_{sm}\cdot c_{om}} \tag{5}$$

$$E_v=\frac{\left|c_s-c_m\right|}{c_m}\times 100\% \tag{6}$$

where:

c_s is simulated data, c_m is the measured data, c_{sm} is the average of the simulated data, c_{om} is the average of the measured data and E_v is relative error between the simulated data and the measured data.

The comparisons of the NMSE of C-type mesh model is the lowest in the four schemes and the three heights which show its higher reliability in simulating the airflow velocity and temperature (Table 4). Therefore, the C-type mesh model is considered adequate for this pigsty.

Table 4

NMSE values in different planes with different grid numbers

	Airflow velocity				Temperature			
	A	B	C	D	A	B	C	D
0.4 m	0.32395	0.11771	0.00599	0.02624	0.05646	0.01511	0.00034	0.00586
1.0 m	0.24143	0.09546	0.00714	0.02368	0.05938	0.02576	0.00126	0.00597
1.6 m	0.21560	0.06061	0.00669	0.02104	0.06052	0.03678	0.00214	0.01182
Average	0.26033	0.09126	0.00661	0.02366	0.05879	0.02588	0.00125	0.00788

- **Temperature numerical simulation in pigsty**

As discovered in Fig.12, the temperature on the plane of Z = 0.81m in the pigsty is not distributed evenly. On the right side (the side with more pigs), the temperature is between 6.45°C and 7.72°C and the average temperature is 6.79 °C, higher than the left side (the side with fewer pigs) since pigs are one of the main heat sources. Meanwhile, the air inlets at the top of the pigsty are near the left side, so, the temperature in this side is lower and the temperatures in the most areas are between 2.64 °C and 5.18 °C, with an average temperature of 4.15 °C. In addition, there are 6 pens in the pigsty, the overall temperature on the right side is close to the outlet and discharged through the negative pressure of the fan, so the temperature in the right pens is higher than the average temperature in the left pens.

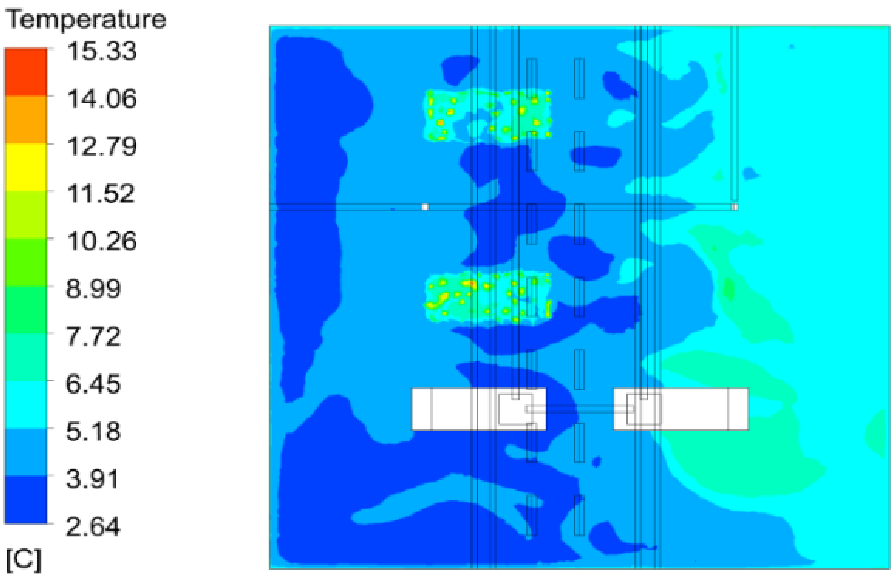

Fig. 12 - Temperature distribution at Z = 0.81m

Fig.13 shows the temperature distribution at Y = 0m, the middle of the longitudinal section of the pigsty. The heat sources in the pigsty mainly come from the heating and the pigs' temperature. The air inlets are located on the upper part of the pigsty, from which the cold air enters. The cold air is heated by the heating in the downward process, then it flows to the pigs. As the other main heat source in the pigsty, the air temperature around the pigs is also improved. With the cold air that continues to move in, most of the heat on the left side enters the manure pit through the slatted floor and is removed by the fans, and the rest of the heat is retained on the upper part of the pigsty due to the turbulence, the temperature is between 6 °C and 9 °C with an average temperature of 6.89 °C. On the right side with fewer pigs, the overall temperature is lower than on the left, except for a small portion of the warmer area around the heating, the temperature is between 3 °C and 6 °C; the average temperature is 4.25 °C.

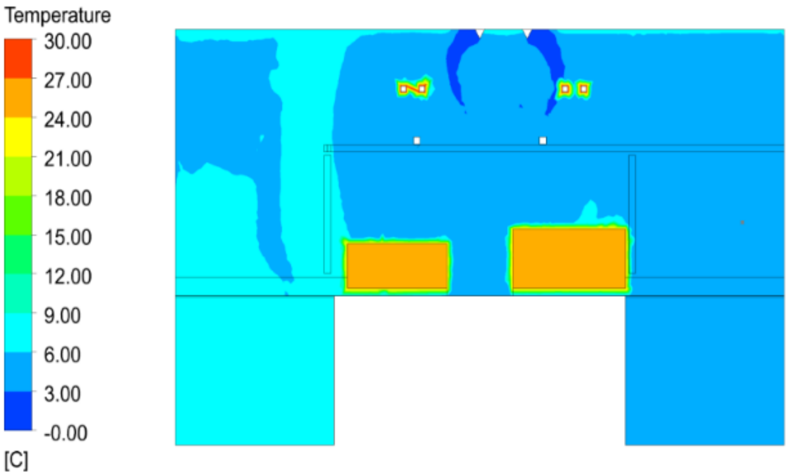

Fig. 13 - Temperature distribution at Y = 0m

- **Airflow numerical simulation in pigsty**

Fig.14 shows the velocity of the airflow distribution at Z = 0.81m. As the figure illustrates, areas with higher airflow velocity are concentrated near the pigs with the maximum value of 0.29 m/s and the other areas is below 0.25 m/s. In addition, the closer the airflow to the outlets, the higher the velocity is, and the uniformity of the airflow gradually increases. The average airflow velocity in this plane is 0.11 m/s. However, the overall airflow uniformity performs poor, which is related to the opening angle of the air inlets and the number of pigs in the pens.

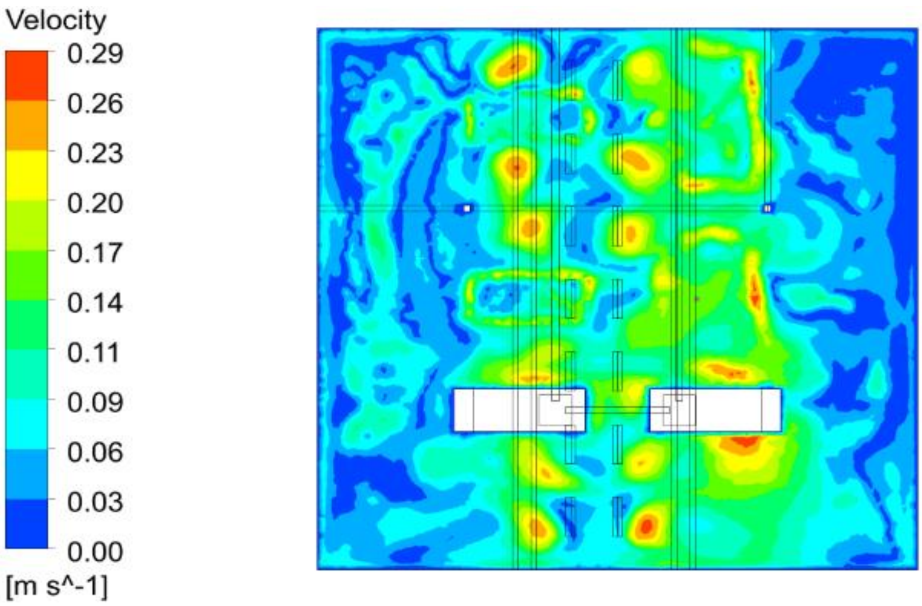

Fig. 14 - Velocity distribution at Z = 0.81m

It can also be seen from Fig.15 that the airflow velocity in the middle of the pigsty at Y= 0 m is between 0.1 m/s and 0.35 m/s, but the airflow velocity around the heating and the large feeding station is between 0m/s and 0.05 m/s due to their obstruction of the airflow. Meanwhile, the airflow velocities both on the left and right sides of the pigsty are all lower, and the airflow is sucked away by the fans in the manure pit through the slatted floor. Although the cold air can remove some harmful gases and toxic particles in the pigsty, it also takes away a lot of heat. As a result, pigs are mainly lying and huddling together on the concrete floor when they are exposed to low temperature which has a great negative impact on pigs' growth since most of the consumed feed is used to maintain body temperature rather than to grow.

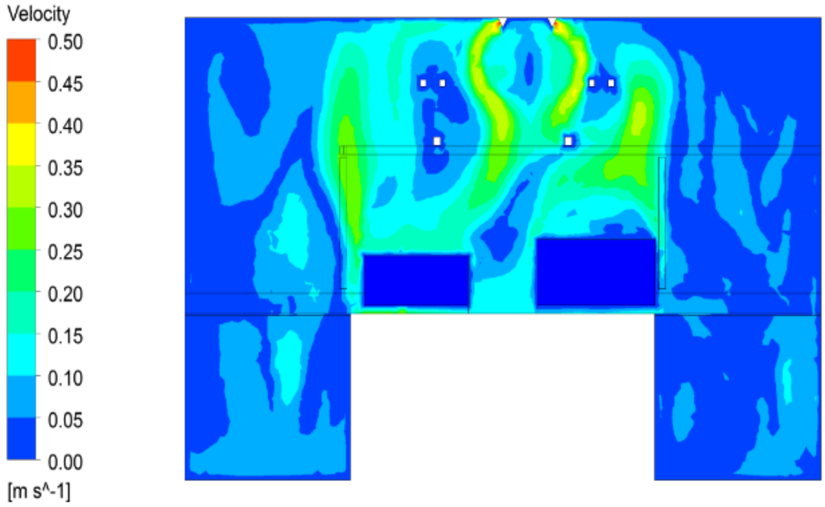

Fig. 15 - Velocity distribution of Y = 0m

CONCLUSIONS

Grid numbers is of great significance to the accuracy of CFD simulation. The average relative error based on C-type mesh model on three different heights of airflow velocity and temperature are 7.1% and 3.8% respectively, the NMSE values are 0.00126 and 0.00669 respectively, which are the best results in all schemes, indicating good agreements between the simulation and the field test results. Moreover, it can be found that if the mesh generation is too sparse (0.27 million), the relative error of airflow velocity and temperature simulation values would be larger, reaching 46.4 and 23.7%. However, the grid numbers are not the more the better, when the mesh generation is too dense (3.14 million), due to the increase of discrete points, the rounding error increases, which leads to the simulation accuracy reduction by 9.9% and 3.8% (compared with 2.09 million). As such, grid independence verification should be carried out before applying the simulation and calculation. Then, the best model with optimal parameters can be used for the CFD simulation in the experimental pigsty. From the distribution diagrams of temperature and airflow velocity, it is easier to see the whole condition inside the pigsty, some suggestions being obtained to improve the welfare of pigs as well as the economic benefit of the pig farm in cold winter. The first is that the overall ventilation of the pigsty can be improved by adjusting the opening angle of the air inlets to avoid cold air flowing directly into pigs' lying areas when the ventilation is needed to remove the harmful gases which is also important for pigs' health. Meanwhile, increasing the number of pigs in the left pens also makes sense since pigs are the other heat source in the pigsty. Furthermore, while decreasing the airflow velocity around the pigs, the airflow velocity on both left and right sides should also be strengthened to create a more balanced and healthier breeding environment.

ACKNOWLEDGEMENT

The research is supported by 12th Five-year National Science and Technology Support Program of China [2014BAD08B05] and Inner Mongolia Autonomous Region Graduate Student Scientific Research Innovation Projects [B2018111948].

RERERENCES

[1] Duan, R., Liu, W., Xu, L., Huang, Y., Shen, X., Lin, C.H., Liu, J., Chen, Q., & Sasanapuri, B. (2015). Mesh type and number for the CFD simulations of air distribution in an aircraft cabin. *Numerical Heat Transfer, Part B: Fundamentals*, *United Kingdom*, *67*, 489–506. https://doi.org/10.1080/10407790.2014.985991

[2] Hong, S.W., Lee, I.B., Seo, I.H., Bitog, J.P., & Kwon, K.S. (2013). Prediction of livestock odour dispersion over complex terrain using CFD technology: Review and simulation study. *Acta Horticulturae, Belgium, 1008,* 29–36. https://doi.org/10.17660/ActaHortic.2013.1008.2

[3] Li, H., Rong, L., Zhang, G. (2018). Numerical study on the convective heat transfer of fattening pig in groups in a mechanical ventilated pig house. *Computers and Electronics in Agriculture, Netherlands, 149*, 90–100. https://doi.org/10.1016/j.compag.2017.08.013

[4] Nielsen, P. V. (2015). Fifty years of CFD for room air distribution. *Building and Environment*, *United Kingdom, 91*, 78–90. https://doi.org/10.1016/j.buildenv.2015.02.035

[5] Ntinas, G.K., Shen, X., Wang, Y., & Zhang, G. (2018). Evaluation of CFD turbulence models for simulating external airflow around varied building roof with wind tunnel experiment. *Building Simulation*, *China, 11,* 115–123. https://doi.org/10.1007/s12273-017-0369-9

[6] Osorio Saraz, J.A., Arêdes Martins, M., Oliveira Rocha, K.S., Silva Machado, N., & Ciro Velasques, H.J. (2013). Use of computational fluid dynamics to simulate temperature distribution in broiler houses with negative and positive tunnel type ventilation systems. *Revista U.D.C.A Actualidad & Divulgación Científica, Brazil,16,* 159-166. https://doi.org/10.31910/rudca.v16.n1.2013.871

[7] Rojano, F., Bournet, P.E., Hassouna, M., Robin, P., Kacira, M., & Choi, C.Y. (2016). Computational modelling of thermal and humidity gradients for a naturally ventilated poultry house. *Biosystems Engineering*, *United States,151,* 273–285. https://doi.org/10.1016/j.biosystemseng.2016.09.012

[8] SeJun Park, Inbok Lee, Sewoon Hong. (2014). New Development of a Straightforward Method of Estimating Age-of-Air Using CFD. *Acta Horticulturae, Belgium, 1037,* 963–969. https://doi.org/10.17660/actahortic.2014.1037.128

[9] Sapounas, A., Dooren, H. J. C., & Smits, M. C. J. (2013). Natural Ventilation of Commercial Dairy Cow Houses: Simulating the Effect of Roof Shape Using CFD, *Acta Horticulturae, Belgium,1008*, 221-228. https://doi.org/10.17660/ActaHortic.2013.1008.29

[10] Wang, X., Zhang, G., & Choi, C.Y. (2018). Effect of airflow speed and direction on convective heat transfer of standing and reclining cows. *Biosystems Engineering, United States, 167*, 87–98. https://doi.org/10.1016/j.biosystemseng.2017.12.011

[11] Yao, J J., Guo, B B., & Ding, W M. (2017). Structural optimization and verification of ventilation system based on CFD simulation of goose house airflow field (基于鹅舍气流场 CFD 模拟的通风系统结构优化与验证). *Transactions of the Chinese Society of Agricultural Engineering, China, 33*(7), 214-220. https://doi.org/10.11975/j.issn.1002-6819.2017.03.029

[12] Yu, G. B., Sun, S., & Tao, W. Q. (2012). Comparative Study on Triangular and Quadrilateral Meshes by a Finite-Volume Method with a Central Difference Scheme, *Numerical Heat Transfer, Part B: Fundamentals, United Kingdom, 62* (4), 243-263. https://doi.org/10.1080/10407790.2012.709416